Human Reproduction vol.14 no.11 pp.2908–2916, 1999

Quantitative near-infrared spectroscopy of cervical dysplasia *in vivo*

R.Hornung[1,2], T.H.Pham[1], K.A.Keefe[1,3], M.W.Berns[1], Y.Tadir[1] and B.J.Tromberg[1,4]

[1]Laser Microbeam and Medical Program (LAMMP), Beckman Laser Institute and Medical Clinic, University of California (Irvine), 1002 Health Sciences Road East, Irvine, CA 92612, USA, [2]Departement Frauenheilkunde, Universitätsspital Zurich, Switzerland [3]Division of Gynecological Oncology, Medical Center, University of California, Irvine, CA, USA

[4]To whom correspondence should be addressed

The aims of this study were: (i) to quantify near-infrared optical properties of normal cervical tissues and high-grade squamous intra-epithelial lesions (H-SIL); (ii) to assess the feasibility of differentiating normal cervical tissues from H-SIL on the basis of these properties; and (iii) to determine how cervical tissue optical properties change following photodynamic therapy (PDT) of H-SIL *in vivo*. Using the frequency domain photon migration technique, non-invasive measurements of normal and dysplastic ecto-cervical tissue optical properties, i.e. absorption (μ_a) and effective scattering coefficients, and physiological parameters, i.e. tissue water and haemoglobin concentration, percentage oxygen saturation (%SO_2), were performed on 10 patients scheduled for PDT of histologically-proven H-SIL. Cervix absorption and effective scattering parameters were up to 15% lower in H-SIL sites compared with normal cervical tissue for all wavelengths studied (674, 811, 849, 956 nm). Following PDT, all μ_a values increased significantly, due to elevated tissue blood and water content associated with PDT-induced hyperaemia and oedema. Tissue total haemoglobin concentration ([TotHb]) and arterio-venous oxygen saturation measured in H-SIL sites were lower than normal sites ([TotHb]: 88.6 ± 35.8 μmol/l versus 124.7 ± 22.6 μmol/l; %SO_2: 76.5 ± 14.7% versus 84.9 ± 3.4%).

Key words: cervix/optical properties/frequency-domain photon migration/haemoglobin spectroscopy/photodynamic therapy

Introduction

The combination of modern screening methods with increasingly effective treatment modalities has led to a dramatic reduction in mortality due to cervical cancer over the past five decades. In the USA, however, 15 700 new cervical cancer cases were diagnosed and 4900 succumbed to their disease in 1996 (Parker *et al.*, 1996). Despite the significant decline in the incidence and mortality of invasive cervical cancer, there has been an increase in the incidence of cervical intra-epithelial neoplasia (CIN), reflecting both improved screening and detection methods and a true increase in the incidence of pre-cancerous lesions of the cervix (Wright *et al.*, 1995). CIN terminology divides cervical cancer precursors into three groups: CIN I, II, III corresponding to mild, moderate and severe (carcinoma *in situ*) dysplasia (Wright *et al.*, 1995). Low-grade squamous intra-epithelial lesions (L-SIL) correspond to CIN I and high-grade SIL (H-SIL) to CIN II and CIN III (Wright *et al.*, 1995). It is estimated that the mortality from cervical cancer will rise by 20% in the next decade unless improvements are made in current screening and detection techniques (Beral and Booth, 1996).

Current screening techniques for CIN and invasive cervical cancer include the single or combined use of exfoliative cytology (Papanicolaou smear) and colposcopy (i.e. the examination of reflected light from the uterine cervix and the adjacent tissues using a low-magnification microscope) (Ferenczy *et al.*, 1988; Ramanujam *et al.*, 1994a). A false negative Papanicolaou smear error rate of 15–55% is associated with insufficient sampling and reading error (Gay *et al.*, 1985; Van Le *et al.*, 1993; Kierkegaard, *et al.*, 1994). Diagnostic accuracy of colposcopic impression in patients with abnormal cervical cytology ranges from 37.5 to 89.9%, while underdiagnosis of microinvasive disease of up to 100% has been reported (Hopman *et al.*, 1995). Hence, there is a strong need for additional diagnostics that could become rapid, 'online' procedures implemented by physicians and nurse practitioners. Overall, this would facilitate more sensitive and cost-effective screening and follow-up of pre-malignant cervical lesions.

In an attempt to fulfil this need, various techniques, such as cervicography (Coibion *et al.*, 1994; Allen *et al.*, 1995) and speculoscopy (Mann *et al.*, 1993; Massad *et al.*, 1993, Lonky *et al.*, 1995) have been developed to visualize benign, premalignant and malignant cervical tissues. Qualitative methods such as cervicography (Coibion *et al.*, 1994; Allen *et al.*, 1995) and speculoscopy (Mann *et al.*, 1993; Massad *et al.*, 1993; Lonky *et al.*, 1995) are readily adaptable to existing standard-of-care instruments. However, these approaches are unlikely to be sufficiently sensitive to the subtle tissue architectural changes characteristic of H-SIL. Consequently, several promising new techniques which provide quantitative measures of intrinsic differences between normal and abnormal cervical tissue have emerged. These include digital image colposcopy (Shafi *et al.*, 1994; Chenoy *et al.*, 1996), polarography (Schneider and Zahm, 1996), fluorescence spectroscopy (Mahadevan *et al.*, 1993; Ramanujam *et al.*, 1994a,b, 1996) and optical coherence tomography (Sergeev *et al.*, 1997).

All of these approaches provide new information regarding tissue function and are in various stages of clinical investigation. With the exception of polarography, each is fundament-

ally sensitive to intrinsic tissue optical properties. As a result, in this work, we report a series of spectroscopic studies designed to quantify the optical properties of cervical tissue *in vivo*. Our goal was to investigate whether the intrinsic optical property differences were detectable under broadly different physiological states. It is expected that this information will help optimize strategies, which rely on optical contrast for identifying and treating dysplasias since the performance of any optical method is ultimately linked to the distribution of endogenous absorbers and scatterers in the cervical stroma/epithelium.

Visible and near-infrared (NIR) diffuse reflectance spectroscopy is typically used to (non-invasively) characterize optical properties of thick tissues *in vivo* (Patterson *et al.*, 1993). Optical properties can be defined quantitatively in terms of absorption and effective scattering parameters, μ_a and μ'_s respectively. These coefficients are, in turn, sensitive to the tissue concentration of light-absorbing molecules and light scattering structures. The primary tissue contributors to NIR light absorption are generally assumed to be haemoglobin [Hb both oxy- (HbO_2) and deoxy-forms], water, fat, cytochromes (cyt), and melanin (Cope, 1991). Light scatterers are tissue structural elements that have a dimension comparable to the optical wavelength (e.g. ~0.6–1 μm), such as cellular components and fibrous materials in the extracellular matrix (e.g. collagen/elastin).

The sensitivity of optical properties to tissue structure and function suggests that differences between normal and diseased tissues may provide a means for assessing the probability that processes such as malignant transformation, inflammation, or infection are occurring. Indeed, previous studies have shown unique scattering and/or absorption signatures associated with dysplastic (Bigio and Mourant, 1997; Perelman *et al.*, 1998), malignant (Fishkin *et al.*, 1997) and benign (Tromberg *et al.*, 1997) tissue transformations. Elastic light scattering (Mourant *et al.*, 1995; Bigio and Mourant, 1997) and fluorescence (Mahadevan *et al.*, 1993; Ramanujam *et al.*, 1994a,b, 1996; Richards-Kortum, *et al.*, 1994) have shown particular promise in their ability to distinguish between cervical structures. Fluorescence has been studied most extensively, and results suggest that quantitative optical property measurements could provide complementary information that would enhance our understanding both of fluorescence data and the transformation process.

Frequency-domain photon migration (FDPM) is a spectroscopic technique capable of quantifying absolute tissue μ_a and μ'_s values. The determination of μ_a and μ'_s at a minimum of three different wavelengths provides a means for quantitative estimation of tissue Hb, HbO_2 and H_2O concentration (Cope, 1991). The instrumentation and theoretical background for FDPM have been described elsewhere (Fishkin *et al.*, 1997; Chance *et al.*, 1998). FDPM-derived optical properties and physiological parameters may be used in a variety of therapeutic and diagnostic settings, including imaging tissue structure and function, monitoring therapy-induced changes of physiology and predicting optical dosimetry for laser based procedures (such as photodynamic therapy).

In previous work, we demonstrated that optical and physiological properties can be measured using FDPM techniques *in vivo* and in model systems (Tromberg *et al.*, 1993, 1996; Fishkin *et al.*, 1997). The present study was designed to determine the sensitivity of FDPM to μ_a and μ'_s changes in tissues containing small, pre-malignant lesions (H-SIL). From these measurements, a better definition of emerging relationships between optical properties and tissue physiological status was attempted. In addition, a description was given of tissue property changes that may occur following a non-invasive photomedical treatment for selective destruction of H-SIL, photodynamic therapy (PDT) (Henderson and Dougherty, 1992; Monk *et al.*, 1997). Although substantial progress has been made in identifying how PDT parameters, e.g. drug dose, drug-light-interval and light dose, could be optimized to produce a tissue-specific effect (Foster *et al.*, 1991; Singh *et al.*, 1991; Foster and Gao, 1992; Sharkey *et al.*, 1993), new methods which dynamically report tissue structural and functional changes are likely to be useful in optimizing treatment efficacy. This appears to be the first clinical study which attempts to measure non-invasively and quantitatively the optical and physiological properties of normal and dysplastic cervical tissue prior to and following PDT.

Materials and methods

Patients

A total of 10 patients were included in the study after written informed consent was obtained. The study was approved by the Human Subject Review Committee of the University of California, USA (IRB#95–567). Patients were referred to our laser clinic with histologically proven H-SIL for treatment of the lesion by means of PDT. Average age was 28 ± 9 years (mean ± SD), nine patients were pre-menopausal, one patient was post-menopausal. Measurements on normal and dysplastic tissues were performed on all 10 patients. The optical properties of seven patients were monitored prior, during and after PDT.

FDPM instruments

A portable, multi-wavelength, high-bandwidth, FDPM instrument was used to perform all the measurements. The instrument is described in detail elsewhere (Madsen *et al.*, 1994a; Tromberg *et al.*, 1996; Fishkin *et al.*, 1997). Briefly, in FDPM the intensity of light incident on an optically turbid sample is modulated at high frequencies, and the diffusely reflected or transmitted signal is measured with a phase-sensitive detection system. Sinusoidally intensity-modulated light propagates through multiple-scattering media with a coherent front, forming photon density waves (PDW) (Fishkin and Gratton, 1991; Tromberg *et al.*, 1993). Wave dispersion is highly dependent on the optical properties of the medium. Thus, measurements of the frequency- or distance-dependent phase and amplitude of PDW can be used to derive scattering (μ'_s) and absorption (μ_a) coefficients in a single measurement. Our FDPM instrument (Figure 1) produces 300 kHz to 1 GHz PDWs in optically turbid media using a network analyser (2) (HP8753C, Hewlett-Packard, Santa Rosa, CA, USA), an avalanche photodiode detector (11) (APD Module C5658; Hamamatsu Corporation Bridgewater, NJ, USA) and four intensity-modulated diode lasers (6) (wavelengths of 674, 811, 849 and 956 nm; PD050-OM; Ortel Corporation, Alhambra, CA, USA). The frequency dependence of PDW phase and amplitude was measured and compared to analytically derived model functions in order to calculate μ_a and μ'_s

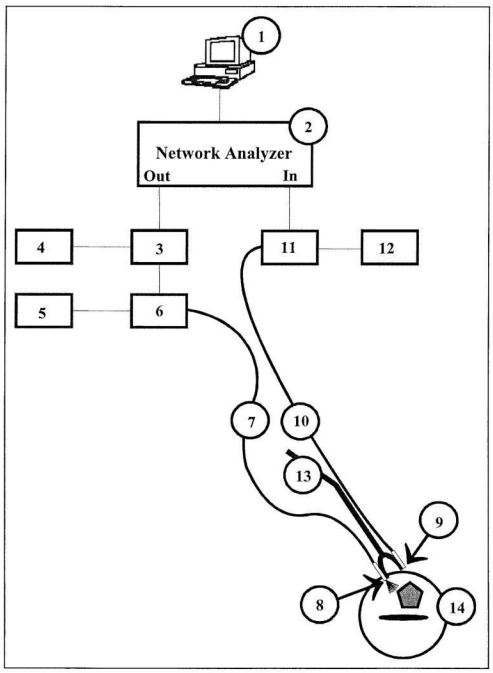

Figure 1. Schematic diagram of the frequency-domain photon migration (FDPM) instrument and cervical probe: computer (1), network analyser (2), bias network (3), dc bias current (4), temperature control (5), four different diode lasers (6) (674 nm, 811 nm, 849 nm, 956 nm), optical fibre for light source (7), lasing tip (8), detecting tip (9), optical fibre for signal detection (10), avalanche photodiode (11), and dc power supply (12). The cervical probe consists of a dilation and curettage (D&C) curette (13) with a modified Y-shaped end instead of the cutting end. The optical fibres (7, 10) were attached to each of the two 9.4 mm separated Y-tips. One fibre was coupled to the laser source and the other fibre was coupled to the light detector. The tip of each of the optical fibres was sealed in transparent resin to one of the Y-tips of the modified D&C curette, and a portion of the length of the fibres was bound together with the length of the curette using a heat shrink plastic tubing. The curette was slightly bent allowing good visualization of the tips during placement of the probe on the cervix (14), shown with high grade squamous intra-epithelial lesions (H-SIL).

parameters. The wavelength-dependence of absorption was used to determine tissue Hb-, HbO_2 and total haemoglobin (TotHb) concentrations, haemoglobin oxygen saturation ($\%SO_2$) and H_2O-concentration. Based on the assumption that the chromophores contributing to μ_a in human tissues are principally Hb, HbO_2 and H_2O, the concentration of each of the three components in the tissue was determined from the FDPM measurements of μ_a at the three different wavelengths. A system of three equations was used to calculate the three unknowns (Fishkin *et al.*, 1997).

The FDPM cervical probe designed for the present study is diagrammatically presented (Figure 1). It was based on a dilation and curettage (D&C) curette (13) with a modified Y-shaped end. The curette was slightly bent allowing good visualization of the tips during placement of the probe. An optical fibre (7, 10) was attached to each of the two 9.4 mm separated Y-tips. One fibre was coupled to the laser source (6) and the other fibre was coupled to the light detector (11). The tip of each of the optical fibres was sealed in transparent epoxy resin to Y-tips of the modified D&C curette, and a portion of the length of the fibres was bound together with the length of the curette using a heat shrink plastic tubing. Prior to and following each use the probe was sterilized in glutaraldehyde (Cydex plus; Johnson & Johnson Medical Inc, Arlington, TX, USA).

Procedure

Prior to any procedure all patients underwent a routine gynaecological check-up in our clinic, including pelvic examination and a thorough colposcopy with application of 5% acetic acid and photo-documentation of the ectocervix performed by an experienced gynaecologist. The ectocervical H-SIL of each patient, previously diagnosed and biopsied by the referring physician, was identified and the probe was placed in a way that the source fibre touched the cervix directly on the centre of the H-SIL and the detection fibre touched the tissue radially towards the outer cervical margin. Gentle pressure was used to ensure a good probe-cervix contact. FDPM measurements were performed on the lesion and repeated with and without replacement of the probe (two measurements in each case). Subsequently an area of colposcopically normal cervical tissue was chosen and FDPM measurements were repeated, this time with both source and detector fibres entirely in contact with the normal cervical tissue.

After the initial FDPM measurements were performed on the cervical lesions and the normal cervical tissue, PDT was initiated in two steps. Firstly, crystallized 5-aminolevulinic acid (ALA) (DUSA Pharmaceuticals, Denville, NJ, USA) was dissolved in Hyskon (Pharmacia, Piscataway, NJ, USA) to a concentration of 200 mg/ml and was buffered to pH 6 with 10 N sodium hydroxide. According to the estimated size of the cervix a cervical cap (25–31 mm) was chosen and filled with 6–12 ml of ALA/Hyskon. The cap was placed similarly to a contraceptive cervical cap. After 90 min, when a sufficient amount of ALA was expected to be converted to the active photosensitizer PpIX (unpublished data), the cap was removed and the cervix was cleaned with gauze. FDPM measurements were then repeated on exactly the same locations as prior to the ALA application. Secondly, by means of a specially designed PDT speculum connected to a laser fibre, laser light (635 nm) generated from an argon-pumped dye laser (Innova 100; Coherent Model 599, Palo Alto, CA, USA) was applied to the lesions. Two patients were treated with 75 J/cm^2, three patients with 100 J/cm^2, and two patients with 125 J/cm^2. The FDPM measurements were repeated 3 min after completing the PDT illumination. The probe was placed in the same position as in all previous measurements.

Data analysis

Average μ_a and μ'_s values were obtained from three single measurements (with and without replacement of the probe) at a given cervical location (either normal cervical tissue or H-SIL) and at a given time (either prior to ALA application, after ALA application, or 3 min after PDT illumination). Normal values obtained from 10 patients are presented as mean $\pm$ SD. Data comparing different types of tissues (i.e. normal versus H-SIL, or CIN II versus CIN III) or data comparing lesions prior and after treatments (i.e. prior versus after application of ALA, prior versus. after PDT illumination) are presented as follows: the optical property ratios from 'H-SIL/normal' or 'treated/untreated' were calculated for every patient. Ratios for every group were averaged and values presented as mean $\pm$ SD. This approach of using ratios allowed us to visualize baseline variability between patients and to quickly overview changes induced by the dysplasia or the treatment (Figures 3–6). However, in order to determine whether these changes were statistically significant, Student's *t*-test (paired or unpaired, as appropriate) was performed using raw optical or physiological data (actual μ_a, μ'_s, and physiological concentration values, not ratios). This comparison allowed us to account for the variability of normal cervical tissues between patients and to address whether optical property changes induced by H-SIL and PDT treatment were significantly different from the expected range of normal values (Table III). $P < 0.05$ was considered to be significant, and $P < 0.005$ as highly significant.

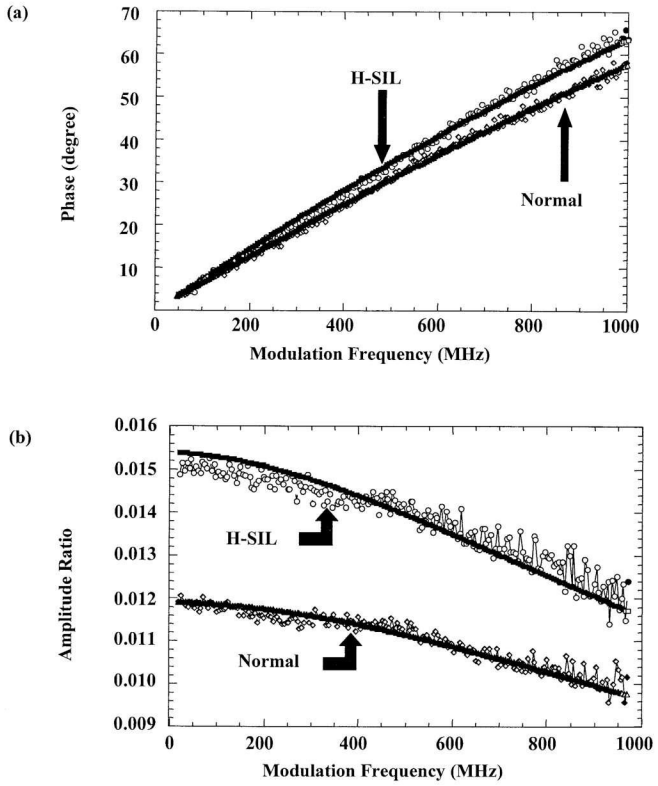

Figure 2. Typical example of frequency-domain photon migration (FDPM) experimental data (○ and ◇) and fit (solid line) from high-grade squamous intra-epithelial lesion (H-SIL, ○) and normal cervical tissue (Normal, ◇). Experimental data were collected at a source-detector separation of 9.45 mm. Phase and amplitude data were simultaneously fit to the semi-infinite, diffusion model functions using the Levenberg–Marquardt non-linear least square algorithm (see text). Plot (**a**) phase (degree) and (**b**) amplitude (amplitude ratio = signal power/source power) data for 674 nm. Typical χ^2 values of simultaneous fits ranged from 2 to 6 per degree of freedom (df).

Results

The absolute absorption (μ_a) and scattering (μ'_s) of normal cervical tissue were determined for four wavelengths (674, 811, 849 and 956 nm), prior to photosensitizer application. Figure 2 shows a typical example of 674 nm FDPM experimental and fitted data from H-SIL and normal cervical tissues. FDPM phase (Figure 2a) and amplitude (Figure 2b) measurements were simultaneously fit to the semi-infinite, diffusion model functions using the Levenberg–Marquardt non-linear least squares algorithm (Spott *et al.*, 1999).

Mean values and SE for μ_a and μ'_s of normal and high-grade (CIN II and III) dysplastic cervical tissue not exposed to photosensitizer or PDT illumination are listed for every wavelength separately in Table I. These values can be summarized as: (i) the range of optical properties for normal and increasing grades of H-SIL; and (ii) the extent of overlap between normal and dysplastic cervical tissues. Physiological parameters were calculated from these values and summarized in Table II. The results show that normal cervical tissue total haemoglobin concentration [TotHb] averages 124.7 ± 22.6 μmol/l (mean ± SD). The oxygenated [HbO_2] and deoxygenated [Hb] components are 16.9 ± 2.8 μmol/l and 107.8 ± 21.7 μmol/l respectively. From these values, it was possible to deduce an average arterio-venous haemoglobin saturation (%SO_2 = [HbO_2]/[TotHb]) of 84.9 ± 3.4 % for all patients. The water concentration [H_2O] was 27 ± 15 mol/l indicating that the measured tissue averages 49% ± 27% water (based on 100% = 55.6 mol/l). Statistical comparisons of [Hb],

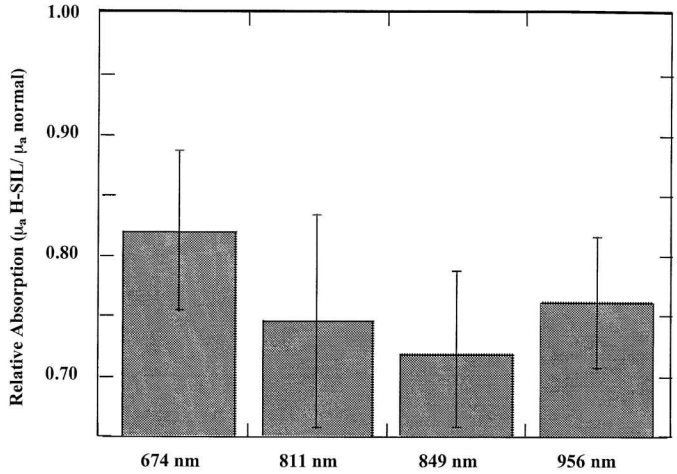

Figure 3. The wavelength dependent light absorption (μ_a) of normal and high-grade squamous intra-epithelial lesions (H-SIL) of the cervix was measured for four wavelengths in 10 patients. Data are presented as mean ± SD of the relative light absorption (relative absorption = μ_a H-SIL/μ_a normal). The ratio allows for a quick overview of changes in optical properties induced by the H-SIL since a relative absorption = 1 indicates no difference between H-SIL and normal tissue. In general H-SIL showed a highly significant decline in light absorption for the investigated wavelengths. Paired Student's *t*-test (n = 10) was performed on the raw absorption values (μ_a) of normal versus H-SIL to determine statistical significance: P = 0.0337, 0.0209, 0.0039, and 0.0028 for 674, 811, 849, and 956 nm respectively, indicating significantly lower light absorption in H-SIL sites for all measured wavelengths.

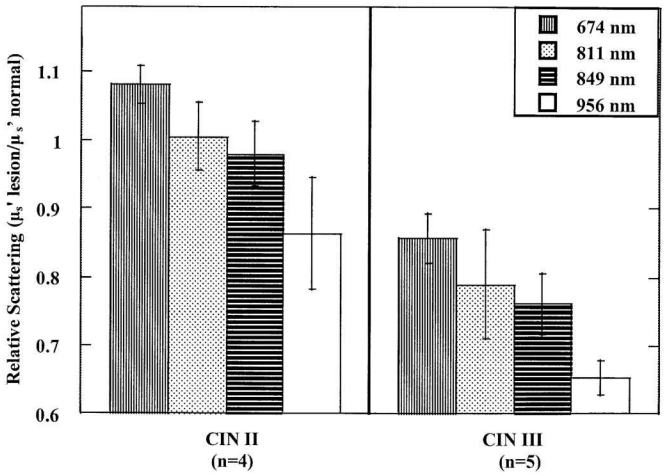

Figure 4. The wavelength dependent relative light scattering (relative scattering = μ'_s lesions/μ'_s normal) is displayed for cervical intra-epithelial neoplasia (CIN) of grade II and III. Data are presented as mean values ± SD of relative scattering, which allows for easy visualization of changes in properties induced by CIN since a relative scattering = 1 indicates no differences between lesions and normal tissues. Light scattering at CIN III sites was significantly higher than light scattering at CIN II and normal sites (see Table III).

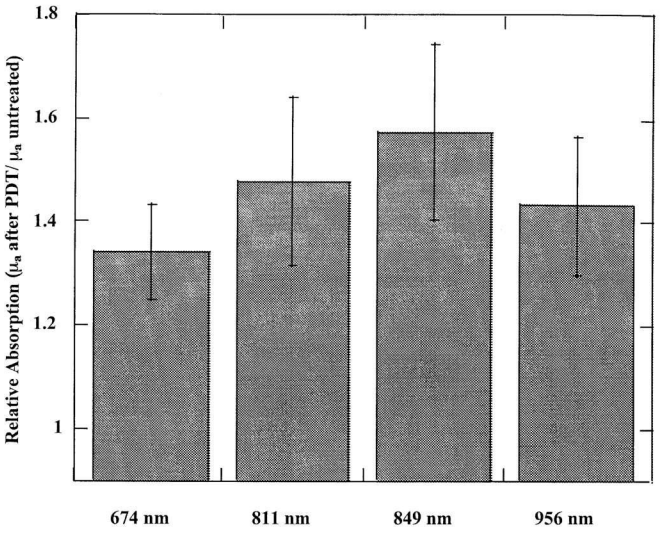

Figure 5. The wavelength dependent relative light absorption (relative absorption = μ_a after PDT/μ_a untreated) of high-grade squamous intra-epithelial lesions (H-SIL) was measured in seven patients prior to (untreated) and after photodynamic therapy (PDT). The ratio allows for a quick overview of changes in optical properties induced by PDT since a ratio of 1 indicated no difference between treated and untreated. Data are presented as mean values ± SD. Statistical significance was determined using paired Student's *t*-test ($n = 7$) to compare raw μ_a values pre- versus post-PDT at 674, 811, 849, and 956 nm. Results yield $P = 0.0104$, 0.0073, 0.0009, and 0.0156 respectively, indicating that PDT causes absorption to increase at all measured wavelengths.

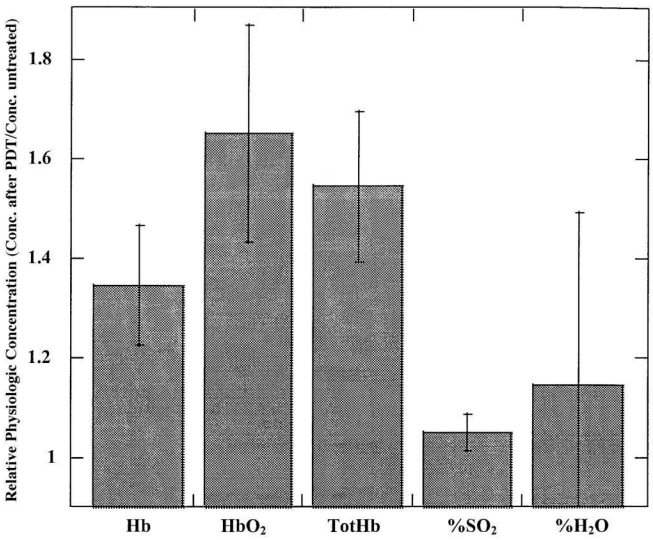

Figure 6. Photodynamic therapy (PDT)-induced changes in the concentrations (Conc.) of physiological parameters were calculated for high-grade squamous intra-epithelial lesions (H-SIL) prior to and 3 min after laser irradiation in seven patients. Physiological parameters (Hb = deoxygenated hemoglobin, HbO_2 = oxygenated haemoglobin, TotHb = total haemoglobin, $\%SO_2$ = oxygen saturation percentage, and $\%H_2O$ = percentage water content) of tissues after PDT treatment were normalized to untreated values (relative conc. = conc. after PDT treatment/conc. untreated). The ratio allows a quick overview of changes in physiological properties induced by PDT since a ratio of 1 indicates no changes between treated and untreated. Data are presented as mean values ± SD. Statistical significance was determined using paired Student's *t*-test ($n = 10$) to compare the concentrations of pre- versus post-PDT physiological properties: $P = 0.2544$, 0.004, 0.003, 0.257, and 0.505 for Hb, HbO_2, total Hb, $\%SO_2$, and $\%H_2O$ content respectively.

$[HbO_2]$, [TotHb], $\%SO_2$, and $\%H_2O$ for normal cervical tissues versus H-SIL gave $P = 0.2365$, 0.0012, 0.0022, 0.0786, and 0.0534 respectively. H-SIL sites had significantly ($P < 0.05$) lower total haemoglobin (88.6 ± 35.8 μmol/l) and oxygenated haemoglobin (73.4 ± 32.6 μmol/l) values compared with normal regions. % SO_2 value (76.5 ± 14.7%) of H-SIL was lower than normal regions, but the difference was not statistically significant.

Figure 3 displays wavelength-dependent relative light absorption of normal cervical tissues and H-SIL (μ_a H-SIL/ μ_a normal). Light absorption in H-SIL was clearly lower than in normal cervical tissues. The reduced light absorption in high-grade dysplastic tissues was seen at all four wavelengths. This suggests that the volume-fraction of blood-perfused tissue was reduced in H-SIL relative to the normal cervical regions (based on the assumption that haemoglobin is the principal absorber at the measured wavelengths). Figure 4 shows that the light scattering parameter (μ'_s) was, in general, lower for H-SIL than normal cervical tissues. Differences in μ'_s for normal cervical tissues versus CIN III were more pronounced than for normal versus CIN II.

Table III summarizes the results of Student's *t*-test ($n = 10$ patients) between mean optical properties for normal sites and each lesion grade (H-SIL, CIN II, CIN III). The absorption coefficient was slightly lower in CIN III versus CIN II (significant at 956 nm). μ_a of CIN II showed a tendency to be lower than μ_a of normal tissue at all four wavelengths, but differences were not significant. μ_a of CIN III was significantly different from μ_a of normal tissue in three out of four investigated wavelengths (811, 849, 956), and H-SIL values were significantly different from normal at all wavelengths. CIN II μ'_s values were comparable with those of normal cervical tissue. However, CIN III scattered light less than CIN II (674, 811, 956), resulting in light scattering values that were significantly lower in CIN III compared with normal sites for all wavelengths. Overall, H-SIL was significantly different from normal at 849 and 956 nm.

FDPM measurements were performed prior to and 90 min following topical application of ALA without appreciable changes in μ_a and μ'_s values. However, 3 min after completing photodynamic therapy (PDT), a dramatic increase in light absorption was observed. Figure 5 shows the wavelength-dependent relative light absorption (μ_a after PDT/μ_a untreated) of seven cervical dysplasias treated with PDT. μ_a increased by ~40% following PDT and mean values were significantly different from untreated dysplastic sites at all four wavelengths ($P < 0.05$). Despite dramatic changes in μ_a, there were no detectable variations in tissue scattering (μ'_s) after PDT. Figure 6 displays the PDT induced relative changes (treated/ untreated) of [Hb], $[HbO_2]$, [TotHb], $\%SO_2$ and $\%H_2O$ of seven patients 3 min after laser irradiation. The calculation of these physiological parameters yields further insight into the PDT-induced pathophysiology. Both total haemoglobin [TotHb] and oxygenated haemoglobin $[HbO_2]$ increased significantly after PDT by

Table I. Measured absorption (μ_a) and scattering (μ'_s) coefficients of normal and dysplastic cervical tissues for four wavelengths. μ_a and μ'_s are in units of mm^{-1}

Optical property	Normal Mean ± SD	CIN II Mean ± SD	CIN III Mean ± SD	H-SIL Mean ± SD
Absorption				
μ_a at 674 nm	0.019 ± 0.004	0.015 ± 0.004	0.016 ± 0.006	0.016 ± 0.005
μ_a at 811 nm	0.027 ± 0.009	0.020 ± 0.009	0.020 ± 0.009	0.020 ± 0.009
μ_a at 849 nm	0.034 ± 0.010	0.023 ± 0.010	0.025 ± 0.011	0.024 ± 0.011
μ_a at 956 nm	0.057 ± 0.012	0.044 ± 0.013	0.043 ± 0.012	0.043 ± 0.013
Scattering				
μ'_s at 674 nm	0.905 ± 0.153	0.844 ± 0.047	0.841 ± 0.125	0.843 ± 0.101
μ'_s at 811 nm	0.558 ± 0.140	0.490 ± 0.087	0.468 ± 0.137	0.477 ± 0.120
μ'_s at 849 nm	0.611 ± 0.116	0.524 ± 0.057	0.503 ± 0.118	0.512 ± 0.098
μ'_s at 956 nm	0.498 ± 0.037	0.389 ± 0.097	0.341 ± 0.072	0.360 ± 0.086

CIN II = cervical intra-epithelial neoplasia (moderate); CIN III = cervical intra-epithelial neoplasia (severe carcinoma *in situ*); H-SIL = high-grade squamous intra-epithelial lesions.

Table II. Comparison of physiological properties of normal cervical tissues with high-grade squamous intra-epithelial lesions (H-SIL)

Physiological property[a]	Normal Mean ± SD	H-SIL Mean ± SD	Student's *t*-test[b] *P* value
[Hb] (μmol/l)	16.9 ± 2.8	15.2 ± 5.1	0.2365
[HbO_2] (μmol/l)	107.8 ± 21.7	73.4 ± 32.6	0.0012
[TotHb] (μmol/l)	124.7 ± 22.6	88.6 ± 35.8	0.0022
$\%SO_2$ ($\%SO_2$ = [HbO_2]/ [TotHb])	84.9 ± 3.4	76.5 ± 14.7	0.0786
$\%H_2O$ (100% =55.6 mol/l)	54.3 ± 14.9	45.7 ± 11.7	0.0534

[a]Physiological properties were calculated from tissue μ_a values (see text).
[b]Paired Student's *t*-test for normal tissues versus H-SIL (n = 10) was used.
Hb = deoxygenated haemoglobin; HbO_2 = oxygenated haemoglobin; TotHb = total haemoglobin; $\%SO_2$ = oxygen saturation.

Table III. Results of Student's *t*-test comparison of optical properties (μ_a, μ'_s) measured at the four wavelengths from normal and tissues with cervical intra-epithelial neoplasia (CIN)

Optical property	Normal versus CIN II[a]		Normal versus CIN III[a]		CIN II versus CIN III[b]		Normal versus H-SIL[a]	
	P value	Significance level[c]	*P* value	Significance level[c]	*P* value	Significance level[c]	*P* value	Significance level[c]
Absorption								
μ_a at 674 nm	0.098	NS	0.078	NS	0.304	NS	0.034	<0.05
μ_a at 811 nm	0.061	NS	0.035	<0.05	0.278	NS	0.021	<0.05
μ_a at 849 nm	0.054	NS	0.011	<0.05	0.226	NS	0.004	<0.005
μ_a at 956 nm	0.161	NS	0.002	<0.005	0.044	<0.05	0.003	<0.005
Scattering								
μ'_s at 674 nm	0.066	NS	0.015	<0.05	0.004	<0.005	0.161	NS
μ'_s at 811 nm	0.942	NS	0.041	<0.05	0.104	NS	0.063	NS
μ'_s at 849 nm	0.668	NS	0.003	<0.005	0.018	<0.05	0.011	<0.05
μ'_s at 956 nm	0.185	NS	0.002	<0.005	0.032	<0.05	0.001	<0.005

[a]Paired Student's *t*-test comparison between normal tissues versus lesions (CIN II, CIN III, H-SIL).
[b]Unpaired *t*-test between CIN II versus CIN III.
[c]Level of significance is listed next to the *P* value to highlight the test result; NS = not significant; P <0.05 = significant; P < 0.005 = highly significant.

~60%. Water content, as assayed by FDPM, increased ~20% immediately post-PDT, but showed wide inter-patient variation. Absolute concentrations for [Hb], [HbO_2] and [TotHb] (μmol/l) are displayed in Figure 7 as a function of the optical dose (J/cm^2). Although only a small number of patients was studied in each group (n = 2 for 75 J/cm^2, n = 3 for 100 J/cm^2, n = 2 for 125 J/cm^2) the dose-dependent tissue reaction can be seen. Increasing the optical dose for PDT elevates all three of these physiological parameters. No significant changes in tissue $\%SO_2$ values were observed post-PDT.

Discussion

The reduction of mortality from cervical cancer during the last 50 years is generally attributed to advances in cytological screening. Yet a substantial number of women are still dying

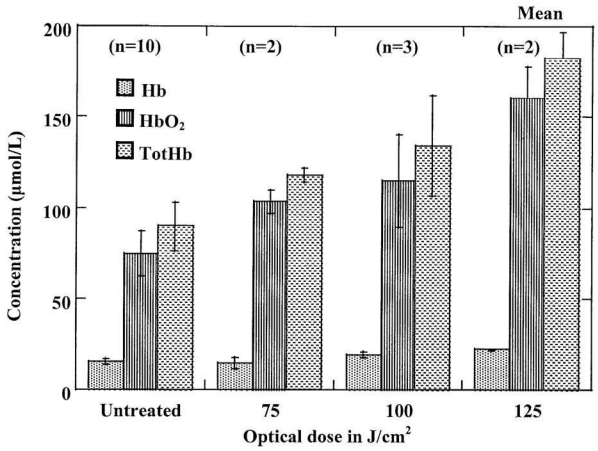

Figure 7. Concentration (µmol/l) of deoxygenated haemoglobin [Hb], oxygenated haemoglobin [HbO_2] and total haemoglobin [TotHb] calculated and displayed as a function of the optical dose (J/cm^2) of laser light applied to induce photodynamic therapy (PDT) on high grade squamous intra-epithelial lesions (H-SIL) of seven patients. Data are presented as mean ± SD.

of cervical cancer in countries in which cytological screening is well-established (Schneider and Zahm, 1996). As well as the increasing incidence of cervical neoplasias and possible insufficient compliance with the screening programme, false negative rates for Papanicolaou smears range from 15 to 55% (Gay *et al.*, 1985) and are as high as 65% for pre-invasive disease (Pairwuti, 1991). Detection of pre-invasive or early invasive disease can be improved by higher reliability of cytology as well as by development of additional screening technology.

NIR photon migration spectroscopy has been developed experimentally and clinically for non-invasive monitoring of tumours and normal tissue physiology (De Blasi *et al.*, 1993; Gratton *et al.*, 1995; Pollard *et al.*, 1996; Fishkin *et al.*, 1997; Tromberg *et al.*, 1997). Photon migration in highly scattering tissues gives optical pathlengths that are dependent upon absorption and scattering parameters (μ_a and μ'_s). Separation and quantification of these parameters can be used to calculate the concentration of principal tissue absorbers in the red and NIR spectral region (i.e. haemoglobin and water) (Fishkin *et al.*, 1997). Substantial interest has been generated in the use of optical techniques for locating, identifying and monitoring malignant transformations (Fishkin *et al.*, 1997; Tromberg *et al.*, 1997; Fantini *et al.*, 1998). Although few attempts have been made to investigate the capability of NIR spectroscopy to detect precancerous lesions on the uterine cervix, other optical methods, such as fluorescence spectroscopy, appear to have substantial promise in this area. Since FDPM is a quantitative optical method, it may provide insight into the complex relationships between optical and physiological properties that form the basis of any successful cervical 'optical biopsy.'

Here, the in-vivo measurements of light absorption (μ_a) and scattering (μ'_s) parameters for normal and high-grade dysplastic cervical tissues are reported. Our normal cervical tissue results are in excellent agreement with the data from other authors (Madsen *et al.*, 1994b) who determined ex-vivo optical properties of uterine tissue at 635 nm. These data provide a baseline measure of normal tissue properties and made it possible to evaluate the impact of pathology (H-SIL) and therapeutic treatments (PDT).

All four optical wavelengths employed in their study showed substantially lower light absorption in H-SIL than in normal cervical tissue. Differences in μ_a between normal and H-SIL sites can be understood in terms of cervical physiology. Normal cervix consists of a 0.5 mm thick (Coleman and Evans, 1988) non-keratinized squamous epithelium with underlying connective tissue. The dimensions of CIN most likely increase by cellular proliferation, which is strongly correlated with the mitotic activity and severity of CIN. Abdul-Karim found a mean maximal depth of 0.93 mm for CIN II and a mean maximal depth of 1.35 mm for CIN III (Abdul-Karim *et al.*, 1982). Thus, on top of a vascularized stroma, the dysplastic growth adds a layer of non-vascularized tissue up to three times thicker than the original normal epithelial layer. Hence, in the H-SIL region, less light can be absorbed by haemoglobin per unit volume of optically probed cervical tissue. Consequently, the measurements of [TotHb] in H-SIL sites were significantly lower than normal (88.6 ± 35.8 versus 124.7 ± 22.6 µmol/l). $\%SO_2$ values were also lower in H-SIL (76.5 ± 14.7 versus 84.9 ± 3.4%) due to the fact that oxygen extraction in lesion-containing tissues is greater than in normal tissues. This effect can be understood in terms of the enhanced metabolic requirements of dysplastic cells as well as the increased oxygen extraction that typically accompanies low blood-volume flow (i.e. low [TotHb]) regions. In normal, high volume flow rate cervix, oxygen extraction demands are less and, as a result, [TotHb] and $\%SO_2$ are high (124.7 ± 22.6 µmol/l and 84.9 ± 3.4% respectively).

Table III and Figure 4 results also show significant differences between grades of dysplasia. Although only a limited number of moderate and severe dysplasias were investigated, CIN II and CIN III seem to have a specific pattern of optical properties. Both CIN II and CIN III showed reduced light absorption relative to normal cervical tissue and mean CIN III absorption was less than CIN II.

Interestingly, there were no significant differences between CIN II light scattering parameters (μ'_s) and normal tissues, while CIN III exhibited substantially lower scattering at all four wavelengths (than in normal tissues). If light scattering within cervix is dominated by stromal collagen, as it is for skin (i.e. dermal connective tissue) (Anderson and Parrish, 1982), the reduced μ'_s values from dysplastic cervical tissue may be explained in a similar way as absorption effects. Here, the thickened H-SIL leads to a shift of the epidermis/stromal fraction in favour of the epithelium. Hence the sub-epithelial structures (i.e. the collagen fibres) underlying a high-grade dysplasia would contribute less to the total light scattering.

Despite this view, the precise origin of light signals remitted from complex tissues is not well understood. Previous work has shown that for probes employing large source-detector separations (e.g. >2 cm), FDPM measurements are insensitive to optical properties of superficial layers (e.g. <4 mm) (Franceschini *et al.*, 1998). Because a cervical probe with a relatively small source-detector separation (9.4 mm) was

employed, it is likely that our mean depth sensitivity is ~3 mm (B.J.Tromberg, unpublished data). Although measurements in this geometry are likely to be influenced by upper layer epithelial changes, it is beyond the scope of this work to fully characterize the relative contributions of epithelial and stromal layers to the total signal. Thus, two alternative explanations of signal origin can be posulated. First, if superficial layer contributions range from minor to negligible, then the decreased μ_a and μ'_s values principally reflect H-SIL stromal changes. Presumably, these optical properties follow from reductions in collagen and blood content averaged over the entire volume of cervical tissue probed. Second, model fits to FDPM data assume the medium to be semi-infinite and homogeneous. In reality, the presence of H-SIL appears to introduce a well-defined upper cervical layer. Depending on the thickness and optical property contrast of this structure, data fits to the homogeneous photon diffusion model could yield inaccuracies in the recovered optical properties. Nevertheless, the impact of H-SIL and PDT on the measurements (both raw data and calculated parameters) was clear. The appearance, progression, and treatment of cervical disease perturbed normal tissue optical properties. These results were easily detected despite inter-patient variability and can be explained in terms of understandable physiology.

Cervical examination by means of FDPM offers not only the possibility of quantitative diagnosis of pre-malignant disease, it also provides information about tissue optics and PDT-induced tissue reactions. Treatment of cervical pathology employing laser light, such as carbon dioxide laser-vaporization, is routinely used to eradicate diseased cervical tissues (Bekassy, 1997). The patients of the present study underwent a novel laser based treatment modality, PDT (Muroya *et al.*, 1996; Monk *et al.*, 1997). The results show that FDPM is sensitive to PDT-induced hyperaemia and oedema in a light dose-dependent fashion (Figure 7). This observation is consistent with previous studies that describe a combination of processes including vessel stasis, permeability alterations, and haemorrhage following PDT (Orenstein *et al.*, 1990; Fingar *et al.*, 1997). Interestingly, tissue scattering changes were not detectable acutely following irradiation, suggesting no major short-term alterations to structural matrix. In addition, no changes in absorption were detected following ALA application due to the fact that the concentration of PpIX (the photo-active metabolite of ALA) in H-SIL exhibits negligible absorption (at 674, 811, 849, 956 nm) compared with other tissue chromophores. However, using other photosensitizers with different absorption peaks or employing additional FDPM wavelengths may allow for direct monitoring of cervical drug uptake. Overall, the treatment-induced tissue response suggests that quantitative optical monitoring strategies may be useful in optimizing PDT efficacy. However, substantial work remains to be carried out to relate time-dependent tissue optical changes with clinical outcome.

In conclusion, the present work has assessed the capability of frequency domain photon migration to characterize normal and high-grade dysplastic cervical tissues based on their optical properties. We have shown that normal cervical tissues can be distinguished from H-SIL and PDT-treated sites, based on both absorption and scattering contrast. Optical property changes can be explained in terms of reasonable structural and functional changes that occur during dysplastic disease progression. However, the precise origin of the measured decrease in absorption and scattering signals is not well understood. Further improvements in FDPM instrumentation and computational models are expected to improve the sensitivity, specificity, and accuracy of optical property measurements in heterogeneous layered structures. Eventually, it is expected that these and related technological advances will stimulate the development of practical quantitative 'optical biopsy' approaches to cervical diagnostics. Finally, since both absorption and scattering parameters are recorded, other possible applications include monitoring processes that involve perfusion and matrix changes, such as cervical ripening during pregnancy and the effects of hormone therapy.

Acknowledgements

This work was supported by the National Institutes of Health (NIH) Laser Microbeam and Medical Program (grant #RR-01192), NIH #R29-GM50958, Department of Energy (DOE #DE-FG03-91ER61227), and Office of Naval Research (ONR #N00014–91-C-0134). T.H. Pham is grateful for the support from the Whitaker Foundation Biomedical Engineering Graduate Fellowship.

References

Abdul-Karim, F.W., Fu, Y.S., Reagan, J.W. *et al.* (1982) Morphometric study of intraepithelial neoplasia of the uterine cervix. *Obstet. Gynecol.*, **60**, 210–214.

Allen, D.G., Ashton, P., Wintle, M. *et al.* (1995) The use of cervicography in the follow-up of cervical intraepithelial neoplasia treated by CO_2 laser. *Aust. N.Z. J. Obstet. Gynaecol.*, **35**, 349–350.

Anderson, R. and Parrish, J. (1982) Optical properties of human skin. In Regan, J. and Parrish, J. (eds), *The Science of Photomedicine*. Plenum Press, London, UK.

Bekassy, Z. (1997) Long-term follow-up of cervical intraepithelial neoplasia treated with minimal conization by carbon dioxide laser. *Lasers Surg. Med.*, **20**, 461–466.

Beral, V. and Booth, M. (1986) Predictions of cervical cancer incidence and mortality in England and Wales. [Letter.] *Lancet*, **i**, 495.

Bigio, I.J. and Mourant, J.R. (1997) Ultraviolet and visible spectroscopies for tissue diagnostics: fluorescence spectroscopy and elastic-scattering spectroscopy. *Phys. Med. Biol.*, **42**, 803–814.

Chance, B., Cope, M., Gratton, E. *et al.* (1998) Phase measurement of light absorption and scatter in human tissue. *Rev. Sci. Instrum.*, **69**, 3457–3481.

Chenoy, R., Billingham, L., Irani, S. *et al.* (1996) The effect of directed biopsy on the atypical cervical transformation zone: assessed by digital imaging colposcopy. *Br. J. Obstet. Gynaecol.*, **103**, 457–462.

Coibion, M., Autier, P., Vandam, P. *et al.* (1994) Is there a role for cervicography in the detection of premalignant lesions of the cervix uteri? *Br. J. Cancer*, **70**, 125–128.

Coleman, D. and Evans, D. (1988) Biopsy pathology and cytology on the cervix. In Gottlieb, L., Neville, A., Walker, F. (eds), *Biopsy Pathology Series*. Chapman and Hall, London, UK.

Cope, M. (1991) *The Development of a Near Infrared Spectroscopy System and its Application for Non Invasive Monitoring of Cerebral Blood and Tissue Oxygenation in the Newborn Infant*. University College London, Ph.D. Thesis.

De Blasi, R.A., Cope, M., Elwell, C. *et al.* (1993) Noninvasive measurement of human forearm oxygen consumption by near infrared spectroscopy. *Eur. J. Appl. Physiol.*, **67**, 20–25.

Fantini, S., Walker, S.A., Franceschini, M.A. *et al.* (1998) Assessment of the size, position, and optical properties of breast tumors *in vivo* by noninvasive optical methods. *Appl. Opt.*, **37**, 1982–1989.

Ferenczy, A., Hilgarth, M., Jenny, J. *et al.* (1988) The place of colposcopy and related systems in gynecologic practice and research [editorial] [see comments]. *J. Reprod. Med.*, **33**, 737–738.

Fingar, V.H., Wieman, T.J. and Haydon, P.S. (1997). The effects of thrombocytopenia on vessel stasis and macromolecular leakage after photodynamic therapy using photofrin. *Photochem. Photobiol.*, **66**, 513–517.

Fishkin, J.B. and Gratton, E. (1993). Propagation of photon-density waves in strongly scattering media containing an absorbing semi-infinite plane bounded by a straight edge. *J. Opt. Soc. Am., A, Opt. Image Sci.*, **10**, 127–140.

Fishkin, J., Coquoz, O., Anderson, E. *et al.* (1997) Frequency-domain photon migration measurements of normal and malignant tissue optical properties in a human subject. *Appl. Opt.*, **36**, 10–20.

Foster, T.H. and Gao, L. (1992) Dosimetry in photodynamic therapy: oxygen and the critical importance of capillary density. *Radiat. Res.*, **130**, 379–383.

Foster, T.H., Murant, R.S., Bryant, R.G. *et al.* (1991) Oxygen consumption and diffusion effects in photodynamic therapy. *Radiat. Res.*, **126**, 296–303.

Franceschini, M.A., Fantini, S., Paunescu, L.A.. *et al.* (1998) Influence of a superficial layer in the quantitative spectroscopic study of strongly scattering media. *Appl. Opt.*, **37**, 7447–7458.

Gay, J.D., Donaldson, L.D. and Goellner, J.R. (1985) False-negative results in cervical cytologic studies. *Acta Cytol.*, **29**, 1043–1046.

Gratton, G., Fabiani, M., Friedman, D. *et al.* (1995) Rapid changes of optical parameters in the human brain during a tapping task. *J. Cogn. Neurosci.*, **7**, 446–456.

Henderson, B.W. and Dougherty, T.J. (1992) How does photodynamic therapy work? *Photochem. Photobiol.*, **55**, 145–157.

Hopman, E.H., Voorhorst, F.J., Kenemans, P. *et al.* (1995) Observer agreement on interpreting colposcopic images of CIN. *Gynecol. Oncol.*, **58**, 206–209.

Kierkegaard, O., Byrjalsen, C., Frandsen, K.H. *et al.* (1994) Diagnostic accuracy of cytology and colposcopy in cervical squamous intraepithelial lesions. *Acta. Obstet. Gynecol. Scand.*, **73**, 648–651.

Lonky, N.M., Mann, W.J., Massad, L.S. *et al.* (1995) Ability of visual tests to predict underlying cervical neoplasia. Colposcopy and speculoscopy. *J. Reprod. Med.*, **40**, 530–536.

Madsen, S., Anderson, E., Haskell, R. *et al.* (1994a) Portable, high-bandwidth frequency-domain photon migration instrument for tissue spectroscopy. *Opt. Lett.*, **19**, 1934–1936.

Madsen, S., Wyss, P., Svaasand, L. *et al.* (1994b) Determination of the optical properties of the human uterus using frequency-domain photon migration and steady-state techniques. *Phys. Med. Biol.*, **39**, 1191–1202.

Mahadevan, A., Mitchell, M.F., Silva, E. *et al.* (1993) Study of the fluorescence properties of normal and neoplastic human cervical tissue. *Lasers Surg. Med.*, **13**, 647–655.

Mann, W., Lonky, N., Massad, S. *et al.* (1993) Papanicolaou smear screening augmented by a magnified chemiluminescent exam. *Int. J. Gynaecol. Obstet.*, **43**, 289–296.

Massad, L.S., Lonky, N.M., Mutch, D.G. *et al.* (1993) Use of speculoscopy in the evaluation of women with atypical Papanicolaou smears. Improved cost effectiveness by selective colposcopy. *J. Reprod. Med.*, **38**, 163–169.

Monk, B.J., Brewer, C., VanNostrand, K. *et al.* (1997) Photodynamic therapy using topically applied dihematoporphyrin ether in the treatment of cervical intraepithelial neoplasia. *Gynecol. Oncol.*, **64**, 70–75.

Mourant, J.R., Bigio, I.J., Boyer, J. *et al.* (1995) Spectroscopic diagnosis of bladder cancer with elastic light scattering. *Lasers Surg. Med.*, **17**, 350–357.

Muroya, T., Suehiro, Y., Umayahara, K. *et al.* (1996) Photodynamic therapy (PDT) for early cervical cancer. *Japn. J. Cancer Chemoth.*, **23**, 47–56.

Orenstein, A., Nelson, J.S., Liaw, L.H.L. *et al.* (1990) Photochemotherapy of hypervascular dermal lesions – a possible alternative to photothermal therapy. *Laser Surg. Med.*, **10**, 334–343.

Pairwuti, S. (1991) False-negative Papanicolaou smears from women with cancerous and precancerous lesions of the uterine cervix. *Acta Cytol.*, **35**, 40–46.

Parker, S.L., Tong, T., Bolden, S. *et al.* (1996) Cancer statistics 1996 [see comments]. *CA Cancer J. Clin.*, **46**, 5–27.

Patterson, M., Pogue, B. and Wilson, B. (1993) Part 4. In Müller, B.C., Alfano, R., Arridge, S. *et al.* (eds), *Medical Optical Tomography: Functional Imaging and Monitoring.* Vol. IS11. SPIE Opt. Eng. Press, Washington, USA.

Perelman, L.T., Backman, V., Wallace, M. *et al.* (1998) Observation of periodic fine structure in reflectance from biological tissue: A new technique for measuring nuclear size distribution. *Phys. Rev. Lett.*, **80,** 627–630.

Pollard, V., Prough, D.S., DeMelo, A.E. *et al.* (1996) Validation in volunteers of a near-infrared spectroscope for monitoring brain oxygenation *in vivo*. *Anesth. Analg.*, **82**, 269–277.

Ramanujam, N., Mitchell, M.F., Mahadevan, A. *et al.* (1994a) *In vivo* diagnosis of cervical intraepithelial neoplasia using 337-nm-excited laser-induced fluorescence. *Proc. Natl. Acad. Sci. USA*, **91**, 10193–10197.

Ramanujam, N., Mitchell, M.F., Mahadevan, A. *et al.* (1994b) Fluorescence spectroscopy: a diagnostic tool for cervical intraepithelial neoplasia (CIN). *Gynecol. Oncol.*, **52**, 31–38.

Ramanujam, N., Mitchell, M.F., Mahadevan, A. *et al.* (1996) Spectroscopic diagnosis of cervical intraepithelial neoplasia (CIN) *in vivo* using laser-induced fluorescence spectra at multiple excitation wavelengths. *Lasers Surg. Med.*, **19**, 63–74.

Richards-Kortum, R., Mitchell, M.F., Ramanujam, N. *et al.* (1994) *In vivo* fluorescence spectroscopy: potential for non-invasive, automated diagnosis of cervical intraepithelial neoplasia and use as a surrogate endpoint biomarker. *J. Cell Biochem. Suppl.*, **19**, 111–119.

Sergeev, A., Gelikonov, V., Gelikonov, G. *et al.* (1997) *In vivo* endoscopic OCT imaging of precancer and cancer states of human mucosa. *Optics Express*, **1**, 432–440.

Schneider, A. and Zahm, D.M. (1996) New adjunctive methods for cervical cancer screening. *Obstet. Gynecol. Clin. N. Am.*, **23**, 657–673.

Shafi, M.I., Dunn, J.A., Chenoy, R. *et al.* (1994) Digital imaging colposcopy, image analysis and quantification of the colposcopic image. *Br. J. Obstet. Gynaecol.*, **101**, 234–238.

Sharkey, S.M., Wilson, B.C., Moorehead, R. *et al.* (1993) Mitochondrial alterations in photodynamic therapy-resistant cells. *Cancer Res.*, **53**, 4994–4999.

Singh, G., Wilson, B.C., Sharkey, S.M. *et al.* (1991) Resistance to photodynamic therapy in radiation induced fibrosarcoma-1 and Chinese hamster ovary-multi-drug resistant cells *in vitro*. *Photochem. Photobiol.*, **54**, 307–312.

Spott, T., Pham, T.H., Svaasand, L.O. *et al.* (1999) Quantitative optical parameter determination in Tissues by Diffuse Photon-Density Waves. *SPIE Proceedings 1999*, **3597**, 423–434.

Tromberg, B., Svaasand, L., Tsay, T. *et al.* (1993) Properties of photon density waves in multiple-scattering media. *Appl. Opt.*, **32**, 607–616.

Tromberg, B., Coquoz, O., Fishkin, J. *et al.* (1996) Frequency-domain photon migration (FDPM) measurements of normal and malignant cell and tissue optical properties. *Biomed. Opt. Spectrosc. Diagn.*, **3**, 111–116.

Tromberg, B.J., Coquoz, O., Fishkin, J.B. *et al.* (1997) Non-invasive measurements of breast tissue optical properties using frequency-domain photon migration. *Philos. Trans. R. Soc. Lond. B. Biol. Sci.*, **352**, 661–668.

Van Le, L., Broekhuizen, F.F., Janzer-Steele, R. *et al.* (1993) Acetic acid visualization of the cervix to detect cervical dysplasia. *Obstet. Gynecol.*, **81**, 293–295.

Wright, T., Kurman, R. and Ferenczy, A. (1995) Precancerous lesions of the cervix. In Kurman R. (ed.), *Blaustein's Pathology of the Female Genital Tract.* Springer-Verlag, New York.

Received on March 23, 1999; accepted on August 5, 1999